Channel Reuse Strategies for Indoor Infrared Wireless Communications

Gene W. Marsh, *Member, IEEE,* and Joseph M. Kahn, *Member, IEEE*

Abstract—We examine systems of fixed-channel reuse for base stations in an indoor infrared wireless communication system. The following techniques are compared:

- time-division multiple access (TDMA) using on-off keying (OOK) or pulse-position modulation (PPM);
- frequency-division multiple access (FDMA) using binary phase-shift keying (BPSK) or quadrature phase-shift keying (QPSK);
- code-division multiple access (CDMA) using OOK with direct-sequence spreading by m-sequences or optical orthogonal codes (OOC's).

We define a parameter γ, which equals the signal-to-noise ratio (SNR) for unit optical path gain and is proportional to the square of the transmitted average optical power. Using measured path-loss data, it is found that in a system using hexagonal cells and a reuse factor of three, for cell radii above 3 m, TDMA with OOK or 2-PPM, and CDMA using OOC's all require approximately the same γ to achieve a worst-case bit-error rate (BER) of 10^{-9} within a cell. Using TDMA with 4-PPM results in a 6-dB decrease in the required value of γ. CDMA using m-sequences requires an increase in γ of 5 dB over TDMA using OOK, and FDMA with BPSK requires an increase of 12 dB. For a given reuse factor N in the noise-limited regime, the required value of γ decreases in inverse proportion to N^2 for TDMA schemes and inversely with N for FDMA and CDMA schemes. For cell radii below 3 m, cochannel interference dominates the systems using TDMA, FDMA, and CDMA with an OOC, resulting in an irreducible BER above 10^{-9} at cell radii below 1.5 m. Only CDMA with m-sequences does not develop an irreducible BER, making it the only choice for cell radii below 1.5 m.

Index Terms— Channel reuse, CDMA, FDMA, infrared, local area networks, TDMA, wireless communications.

I. INTRODUCTION

FREE-SPACE infrared systems using direct detection provide significant advantages over radio systems for short-range, high-speed communication [1]–[3]. The available bandwidth is plentiful and unregulated, making it possible to establish links at very high bit rates. Since infrared radiation is blocked by walls and other opaque barriers, there is no interference between cells in different rooms, and links are secure against causal eavesdropping. Furthermore, because the square-law photodetector is many times larger than the infrared wavelength, multipath propagation does not produce fading in a direct-detection system [4]. However, infrared links using nondirected transmitters and receivers are subject to multipath distortion.

In this paper, we consider networks that utilize infrared links to provide wireless access to base stations connected to a wired backbone network. In such a network, multiple-access techniques are required to coordinate uplink transmissions (from the portable units to the base stations). Ideally, one would like to place a single base station in each room of a building. However, because the signal-to-noise ratio (SNR) of a direct-detection receiver is proportional to the square of the received power, a single base station may be unable to cover a large room. Because of the difficulty of constructing optically tunable receivers having a wide field of view, wavelength-division multiplexing of signals is probably not a viable alternative. When multiple base stations are employed in one room, the transmitter wavelength must be shared, and multiple-access techniques must also be used to coordinate downlink transmissions (from the base stations to the portable units) in order to provide seamless coverage. Channel-sharing techniques for these downlinks are the subject of this paper. We do not treat the problem of the uplink design.

Previous works have consisted mainly of a simplified analysis of one particular multiple access scheme. Valadas *et al.* have examined the use of CSMA/CD for infrared local area networks [5]. Elmirghani and Cryan have examined the use of a hybrid pulse-position-modulation/code-division multiple access system [6]. Gfeller *et al.* have determined how path loss and ambient light noise would affect the achievable data rate and connectivity [7].

In this paper, we compare and contrast several reuse strategies for downlink channel sharing, taking into account ambient noise, path loss, and cochannel interference. Because system bandwidth is plentiful, our goal is to optimize the transmitter power required to obtain seamless coverage of a large room. We will see that the efficiency of a reuse strategy within a wireless infrared system is dominated by the physical-layer characteristics of the modulation schemes used to implement that strategy. For simplicity, we restrict ourselves to fixed channel assignment strategies. Dynamic channel assignment would provide improved performance and should be investigated in a future paper.

In Section II, we give bit-error-rate (BER) formulas for time-division multiple access (TDMA) using on-off keying (OOK) or pulse-position modulation (PPM), frequency-division multiple access (FDMA) using binary phase-shift keying (BPSK) or quadrature phase-shift keying (QPSK),
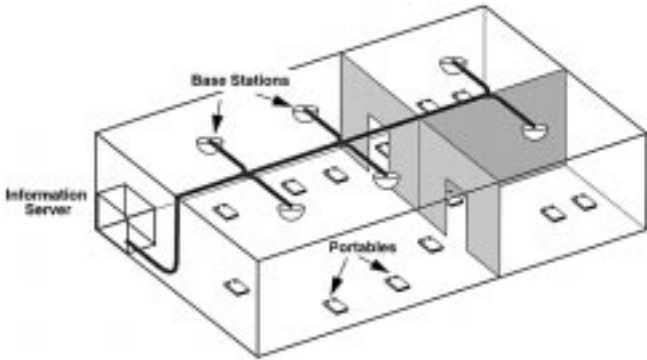
Fig. 1. Local area network utilizing infrared wireless access to a wired backbone.

and code-division multiple access (CDMA) using OOK for direct-sequence spreading, with either m-sequences or optical orthogonal codes (OOC's). Section III compares the various strategies in terms of the average transmitted power required by a cellular scheme to provide a worst-case BER of 10^{-9} over a cell of a given radius. Section IV illustrates how the information obtained from this study can be used in link design. Conclusions are presented in Section V.

II. FIXED CHANNEL ASSIGNMENT STRATEGIES

Fig. 1 shows a local-area network that uses infrared links to provide wireless access to base stations connected to a wired backbone network. In designing the downlinks, our goals are to provide coverage of the entire room, without dead zones, while maximizing the throughput available to users and minimizing the number of base stations and their average transmitted power. The approach we pursue is to divide the downlink transmission into channels, which are to be allocated in a fixed assignment among all the base stations in a room.

The interference between base stations employing different channels should be small. In TDMA, the channels correspond to nonoverlapping time slots. In FDMA, the transmitted signal is divided into nonoverlapping frequency bands. In CDMA using direct-sequence spreading, the channels correspond to different spreading codes. The limited number of channels available means that at least in a large room, some base stations must share the same channel, introducing cochannel interference between these stations. The number of channels used by the system is the reuse factor N.

Some common assumptions are made in all of the schemes presented below. All base stations in the system transmit the same time-averaged optical power, indicated by P_t (in watts). This is defined as

$$P_t = \lim_{T \to \infty} \frac{1}{2T} \int_{-T}^{T} E[s_m(t)] \, dt \qquad (1)$$

where $s_m(t)$ is the signal transmitted by base station m, and the expectation is taken over all possible transmitted bit sequences. We denote by $H_0(\rho)$ (cm^{-2}) the optical gain of the propagation path between a transmitter and a receiver separated by horizontal distance ρ. In all cases, we will assume that ρ is the distance from the desired base station to the desired receiver, that there are M interfering base stations, and

that ρ_m is the distance from the mth interfering base station to the desired receiver. The desired base station will be labeled as $m = 0$. No assumptions are made about the placement of receivers or base stations in this analysis. The constant of proportionality between the received signal irradiance and the detector output photocurrent is given by κ (A · cm^2/W). κ is the product of the receiver optical gain, the transmission of any optical filters used to attenuate ambient light, the detector area, and the detector responsivity. The bit rate of each channel is R_b/N so that the system aggregate bit rate is R_b, and we define $T_b = 1/R_b$. The timing offset for an interfering base station, which is represented by Δ_m for base station m, is assumed to be uniformly distributed over a symbol time. It will be assumed that $\Delta_0 = 0$. The timing offsets are independent of each other and of all other random variables in the system. Ones and zeroes are assumed to be equally likely in the bit stream to be transmitted. Received signals are corrupted by additive noise. This is a combination of shot noise from the ambient light within the room and the thermal noise from the receiver front end. The shot noise in a direct-detection system is often modeled as a signal-dependent, Poisson-rate, photon-counting model. However, in an indoor wireless system, incoherent propagation and the high intensity of the background light makes the shot noise independent of the signal and enables us to model it with extremely high accuracy as a Gaussian white noise with double-sided power spectral density N_0 (A^2/Hz) referred to the input of the preamplifier [2]. N_0 is assumed constant, independent of the receiver's position in the room. We neglect the mean value of this additive noise. To simplify the formulas that follow, we define a parameter γ to be the SNR for unit optical path gain

$$\gamma = \frac{P_t^2 \kappa^2 T_b}{N_0}. \qquad (2)$$

Finally, in the analysis that follows, we assume that the transmission bit rate is low enough so that intersymbol-interference (ISI) effects can by ignored. Some suggestions as to how to relax this assumption will be included in Section IV.

A. Time-Division Multiple Access Techniques

Using a TDMA strategy, each base station is given a time slot during which it can transmit bits. We consider two different modulation schemes that can be used in these transmissions: OOK and PPM.

1) On–Off Keying: In OOK, light is transmitted to encode a one bit, and no light is transmitted to encode a zero bit [2]. We will assume a rectangular pulse shape whose duration equals the bit period. Let a_{mi} be the i_{th} bit transmitted by base station m. Assuming that the N different channels alternate their transmissions on a bit-by-bit basis, the signal transmitted by base station m when it is allocated channel n is

$$s_m^{(n)}(t) = 2NP_t \sum_{i=-\infty}^{\infty} a_{mi}\Pi(\lambda_m(t,i)) \qquad (3)$$

$$\lambda_m(t,i) = \frac{t - (iN + n)T_b - \Delta_m}{T_b} \qquad (4)$$

where

$$\Pi(t) = \begin{cases} 1 & -\frac{1}{2} < t < \frac{1}{2} \\ 0 & \text{otherwise.} \end{cases} \tag{5}$$

We will focus below on base stations using channel $n = 0$. We note that if, instead, the N different channels alternated their transmissions on a block-by-block basis (where any block length could be chosen), our notation would change, but our results would remain the same. The received signal is passed through a unit-energy matched filter, the dc average is removed, and the result is sampled once per bit time. The noise sample associated with symbol i, which is denoted by n_i, is Gaussian with mean zero and variance N_0. Define $\tau_m = \Delta_m/T_b$ so that $\tau_m = (0, 1]$. The noise samples, timing offsets, and data bits are all assumed to be mutually independent. The sampled decision metric for bit i has the form

$$r_i = \sqrt{T_b} N P_t \kappa H_0(\rho)(2a_{0i} - 1)$$
$$+ \sum_{m=1}^{M} \sqrt{T_b} N P_t \kappa H_0(\rho_m) C_m + n_i \tag{6}$$

$$C_m = a_{m,-1}\tau_m + a_{m,0}(1 - \tau_m) - \frac{1}{2}. \tag{7}$$

Without loss of generality, we need only consider bit $i = 0$. The probability of a bit error is then given by

$$P_e = E\left[Q\left(\sqrt{S(\gamma)}\left[1 + \sum_{m=1}^{M} \frac{H_0(\rho_m)}{H_0(\rho)} C_m\right]\right)\right] \tag{8}$$

$$S(\gamma) = N^2 H_0^2(\rho)\gamma \tag{9}$$

where the expectation is taken over all pairs of bits $(a_{m,-1}, a_{m,0})$ and all time offsets τ_m for $m = 1, \cdots, M$, and

$$Q(x) = \frac{1}{\sqrt{2\pi}} \int_x^{\infty} e^{-(y^2/2)} \, dy. \tag{10}$$

2) Pulse-Position Modulation: We restrict our attention to the practical case in which, at each symbol time, L bits are encoded in one of 2^L possible symbols [2], [10]. In this scheme, a symbol time is divided into 2^L time slots of equal width known as chips. In order to transmit symbol k, where $k \in \{0, \cdots, 2^L - 1\}$, a pulse of light is transmitted in the kth chip, and no light is transmitted in any other chip. The pulse is rectangular and has duration equal to the chip period. Let $s_{mi} \in \{0, \cdots, 2^L - 1\}$ be the symbol sent by base station m during symbol time i. Since the data bits into the PPM system are independent and uniformly distributed, the transmitted symbols will be independent and uniformly distributed. Assuming that the N different channels alternate their transmissions on a symbol-by-symbol basis, the signal transmitted by base station m when it is allocated channel n is

$$s_m^{(n)}(t) = 2^L N P_t \sum_{i=-\infty}^{\infty} \Pi(\lambda_m(t,i)) \tag{11}$$

$$\lambda m(t,i) = \frac{t - LT_b\left(iN + n + \frac{s_{mi}}{2^L}\right) - \Delta_m}{\frac{LT_b}{2^L}}. \tag{12}$$

At the receiver, the incoming pulses are convolved with a unit-energy filter matched to the chip pulse and sampled once per chip. If chip l has the largest sample, then symbol l is deemed to have been transmitted. This, in turn, is used to decide which L bits were sent. Let $I(x)$ be an indicator function whose value is one when expression x is true and zero otherwise. Once again, define $\tau_m = \Delta_m/NT_b$. τ_m is uniform over $[0, 1)$. To simplify our notation, we derive two random variables from τ_m. First, define $x_m = \lfloor 2^L \tau_m \rfloor$, and let $y_m = 2^L \tau_m - x_m$. We see that x_m takes on each of the values $\{0, \cdots, 2^L - 1\}$ with probability $1/2^L$, y_m is uniform over $[0, 1)$, and x_m and y_m are independent. Then, it can be shown that the decision metric for base station zero for chip time j and symbol i are given by

$$r_{ij} = \sqrt{2^L LT_b} N P_t \kappa H_0(\rho) A_0 I(s_{00} - j)$$
$$+ \sum_{m=1}^{M} \sqrt{2^L LT_b} N P_t \kappa H_0(\rho_m) C_m + n_{ij} \tag{13}$$

$$C_m = y_m f_m(j-1, l-1) + (1 - y_m) f_m(j, l) \tag{14}$$

$$f_m(j,l) = I(s_{m,-1} + x_m = j + 2^L)$$
$$- I(s_{m,-1} + x_m = l + 2^L)$$
$$+ I(s_{m,0} + x_m = j) - I(s_{m,0} + x_m = l). \tag{15}$$

The n_{ij} are noise samples arising from background light and thermal noise in the receiver and are independent Gaussian random variables with mean zero and variance N_0.

The probability of bit error is difficult to calculate for PPM. Therefore, we resort to calculating the probability of a symbol error P_{se} and then approximating the probability of bit error P_e as $P_e = [2^{L-1}/(2^L - 1)]P_{se}$ [9], [10]. The probability of symbol error is

$$P_{se} = 1 - \frac{1}{2^L} \sum_{k=0}^{2^L-1} E\left[\prod_{\substack{j=0 \\ j \neq k}}^{2^L-1} (1 - Q(\chi))\right] \tag{16}$$

$$\chi = \frac{n_k}{\sqrt{N_0}} + \sqrt{\frac{2^L LT_b}{N_0}} N P_t \kappa H_0(\rho)$$
$$+ \sum_{m=1}^{M} \sqrt{\frac{2^L T_b}{N_0}} N P_t \kappa H_0(\rho_m) C_m \tag{17}$$

where the expectation is taken with respect to the variables x_m, y_m, and the symbol pairs $(s_{m,-1}, s_{m,0})$ for $m = 1, \cdots, M$, and over all values of the Gaussian noise variable n_k. This formula is computationally inefficient and does not yield much to our intuition. For small symbol-error rates, one can expand the product over j and approximate it by keeping only the first-order terms. The resulting approximation for probability of bit error is

$$P_e \approx \frac{1}{2(2^L - 1)}$$
$$\times \sum_{k=0}^{2^L-1} \sum_{\substack{j=0 \\ j \neq k}}^{2^L-1} E\left[Q\left(\sqrt{S(\gamma)}\left[1 + \sum_{m=1}^{M} \frac{H_0(\rho_m)}{H_0(\rho)} C_m\right]\right)\right]$$
$$\tag{18}$$

with

$$S(\gamma) = N^2 2^{L-1} L H_0^2(\rho)\gamma \qquad (19)$$

where the expectation is taken as in (16) and (17). For $L = 1$, these expressions are exact. For $L > 1$, previous work suggests that this approximation should be accurate for BER's below 10^{-2} [10].

B. Frequency-Division Multiple Access Techniques

The FDMA strategies explored below use subcarrier modulation [2], [11]. Each base station is allocated a different frequency. A pulse shape multiplied by a sinusoid of the appropriate frequency is then used to modulate the intensity of the optical signal. Because optical power cannot take on negative values, a dc offset must be added to the signal to ensure that it remains nonnegative. The value of the dc offset depends on the pulse waveform chosen to modulate the sinusoid. The two most popular pulse shapes used in optical subcarrier modulation are rectangular pulses and root-raised-cosine pulses. Since rectangular pulses only provide orthogonality between subcarriers at different frequencies when the different signals are synchronized in time, this study focuses on root-raised-cosine pulses [11]. We consider both BPSK and QPSK-modulated subcarriers.

1) Binary Phase Shift Keying: Let $p_\alpha(t)$ be a root-raised-cosine pulse with excess bandwidth α. In an FDMA system with an aggregate bit rate of R_b and a reuse factor of N, each subcarrier transmits at the reduced data rate R_b/N. Since there is only one symbol per bit in BPSK, R_b/N is also the symbol rate. The pulse shape transmitted is therefore $p_\alpha(t/(NT_b))$. To ensure that unsynchronized signals at different subcarrier frequencies are orthogonal, the signal spectrums must not overlap. This will be true when the subcarriers are separated in frequency by at least $(1+\alpha)/(NT_b)$ (in Hertz). Assuming this spacing, we need only concern ourselves with the M transmitters in the room using the same frequency as the desired base station. Let us call this frequency f_0. Base station m then transmits

$$s_m(t) = \frac{P_t}{C(\alpha)}\left[C(\alpha) + \cos(\omega_m(t))\sum_i (2a_{mi} - 1)\right.$$

$$\left. \cdot\, p_\alpha(\lambda_m(t,i))\right] \qquad (20)$$

$$\omega_m(t) = 2\pi f_0(t - \Delta_m) + \theta_m \qquad (21)$$

$$\lambda_m(t,i) = \frac{t - iNT_b - \Delta_m}{NT_b} \qquad (22)$$

where θ_m is the phase offset for base station m, and $C(\alpha)$ is the dc offset needed to make $s_m(t)$ nonnegative [11]. For $\alpha > 0.4$, $C(\alpha)$ is approximately constant at 1.5. For $\alpha < 0.4$, $C(\alpha)$ increases to infinity. θ_m is uniform over $[0, 2\pi)$. All instances of Δ_m and θ_m are independent of each other. To demodulate the data for base station zero, the receiver multiplies by $\sqrt{2}\cos(2\pi f_0 t + \theta_0)$, passes the result through a unit-energy filter matched to $p_\alpha(t/(NT_b))$, and then samples the result. Without loss of generality, we can take $\theta_0 = 0$.

The output of the matched filter is a raised-cosine pulse with excess bandwidth α, $q_\alpha(t/(NT_b))$, where

$$q_\alpha(t) = -\frac{\sin(\pi t)\cos(\pi\alpha t)}{4\pi\alpha^2 t\left(t^2 - \frac{1}{4\alpha^2}\right)}. \qquad (23)$$

Note that $q_\alpha(t)$ has been defined so that it is zero for $t = \pm 1, \pm 2, \pm 3, \cdots$. Ignoring the dc offset, the decision metrics for bit i are then given by

$$r_i = \sqrt{\frac{NT_b}{2}}\frac{P_t\kappa H_0(\rho)}{C(\alpha)}(2a_{0i} - 1) + n_i$$

$$+ \sqrt{\frac{NT_b}{2}}\frac{P_t\kappa}{C(\alpha)}\sum_{m=1}^{M} I_m \qquad (24)$$

$$I_m = H_0(\rho_m)\cos(\theta_m - 2\pi f_0\Delta_m)$$

$$\times\left(\sum_{j=-\infty}^{\infty}(2a_{mj} - 1)q_\alpha\left(j - i + \frac{\Delta_m}{NT_b}\right)\right) \qquad (25)$$

where the noise samples n_i are independent Gaussian random variables with zero mean and variance N_0. If we let $\phi_m = (\theta_m - 2\pi f_0\Delta_m)\ (\mathrm{mod}\ 2\pi)$, then ϕ_m is uniformly distributed over $[0, 2\pi)$. If we let $\tau_m = \Delta_m/(NT_b)$, then τ_m is uniformly distributed over $[0, 1)$. Further, ϕ_m and τ_m are independent. In this case, the receiver decision metrics become

$$r_i = \sqrt{\frac{NT_b}{2}}\frac{P_t\kappa H_0(\rho)}{C(\alpha)}(2a_{0i} - 1) + n_i$$

$$+ \sqrt{\frac{NT_b}{2}}\frac{P_t\kappa}{C(\alpha)}\sum_{m=1}^{M} I_m \qquad (26)$$

$$I_m = H_0(\rho_m)\cos(\phi_m)$$

$$\times\left(\sum_{j=-\infty}^{\infty}(2a_{mj} - 1)q_\alpha(j - i + \tau_m)\right). \qquad (27)$$

Without loss of generality, we can obtain the probability of a bit error by considering only bit $i = 0$. If r_i is positive, the received bit is declared to be a one; otherwise, the decision is zero. The probability of bit error is then given by

$$P_e = E\left[Q\left(\sqrt{S(\gamma)}\left[1 + \sum_{m=1}^{M} C_m\right]\right)\right] \qquad (28)$$

$$S(\gamma) = \frac{NH_0^2(\rho)\gamma}{2C^2(\alpha)} \qquad (29)$$

$$C_m = \frac{H_0(\rho_m)}{H_0(\rho)}\cos\phi_m\sum_j(2a_{mj} - 1)q_\alpha(j + \tau_m) \qquad (30)$$

where the expectation is taken over all time offsets τ_m, phase offsets ϕ_m, and bit sequences a_{mj} for $m = 1, \cdots, M$ and all j.

2) Quadrature Phase Shift Keying: QPSK modulation is similar to BPSK, except that both in-phase (cosine) and quadrature (sine) carriers are used [11]. We will assume that even bits are transmitted on the in-phase channel, and odd bits are transmitted on the quadrature channel, thus doubling the symbol time. The frequency spacing between adjacent subcarriers is half that required for BPSK, and the dc offset

must be increased to $\sqrt{2}C(\alpha)$. The transmitted signal is given by

$$
s_m(t) = \frac{P_t}{\sqrt{2}C(\alpha)} \left[\sqrt{2}C(\alpha) + \sin(\omega_m(t)) \right.
$$
$$
\cdot \sum_k (2a_{m,2k+1} - 1)p_\alpha(\lambda_m(t,k))
$$
$$
\left. + \cos(\omega_m(t)) \sum_k (2a_{m,2k} - 1)p_\alpha(\lambda_m(t,k)) \right]
$$

(31)

$$
\omega_m(t) = 2\pi f_0(t - \Delta_m) + \theta_m \tag{32}
$$

$$
\lambda_m(t,k) = \frac{t - 2kNT_b - \Delta_m}{2NT_b}. \tag{33}
$$

After demodulation and using assumptions similar to those used for BPSK, we can express the decision metrics i_k and q_k for the in-phase and quadrature bits, respectively, as

$$
i_k = \sqrt{\frac{NT_b}{2}} \frac{P_t \kappa H_0(\rho)}{C(\alpha)} (2a_{0,2k} - 1) + n_{ik}
$$
$$
+ \sqrt{\frac{NT_b}{2}} \frac{P_t \kappa}{C(\alpha)} \sum_{m=1}^M I_m \tag{34}
$$

$$
I_m = H_0(\rho_m) \cos(\phi_m)
$$
$$
\times \left(\sum_{j=-\infty}^{\infty} (2a_{m,2j} - 1)q_\alpha(j - i + \tau_m) \right) \tag{35}
$$

$$
q_k = \sqrt{\frac{NT_b}{2}} \frac{P_t \kappa H_0(\rho)}{C(\alpha)} (2a_{0,2k+1} - 1) + n_{qk}
$$
$$
+ \sqrt{\frac{NT_b}{2}} \frac{P_t \kappa}{C(\alpha)} \sum_{m=1}^M J_m \tag{36}
$$

$$
J_m = H_0(\rho_m) \cos(\phi_m)
$$
$$
\times \left(\sum_{j=-\infty}^{\infty} (2a_{m,2j+1} - 1)q_\alpha(j - i + \tau_m) \right) \tag{37}
$$

where n_{ik} and n_{qk} are the in-phase and quadrature noise samples. These are mutually independent sequences of Gaussian random variables with mean zero and variance N_0. The probability of bit error for this system is given by

$$
P_e = E\left[Q\left(\sqrt{S(\gamma)} \left[1 + \sum_{m=1}^M \frac{H_0(\rho_m)}{H_0(\rho)} C_m \right] \right) \right] \tag{38}
$$

$$
S(\gamma) = \frac{N H_0^2(\rho)\gamma}{2C^2(\alpha)} \tag{39}
$$

$$
C_m = \sum_{k=-\infty}^{\infty} q_\alpha(k + \tau_m)(2a_{m,2k} - 1)\cos(\phi_m)
$$
$$
+ \sum_{k=-\infty}^{\infty} q_\alpha(k + \tau_m)(2a_{m,2k+1} - 1)\sin(\phi_m) \tag{40}
$$

where the expectation is taken over all time offsets τ_m, phase offsets ϕ_m, and bit sequences a_{mj} for $m = 1, \cdots, M$ and all j.

C. Code-Division Multiple Access Techniques

The CDMA techniques considered here rely on direct-sequence spreading [12]. The systems operate at baseband with OOK as the underlying modulation scheme.

1) Direct-Sequence Spreading Using m-Sequences: Let $c_{kj}^{(n)}, j = 0, \cdots, L_c$ and any k be a sequence of binary code bits, which are also known as chips. Note that for each data bit, there are L_c corresponding chips. There will be N different sequences used in this technique. Let $n(m)$ be a function that maps a base station's index into the code sequence it employs. There are many different ways to choose these code sequences. One common choice is the set of maximal-length pseudo-noise (PN) sequences known as m-sequences [12]. If the period of the m-sequences is sufficiently long compared with L_c, then the chips can be conveniently modeled as an infinite sequence of i.i.d. random variables chosen uniformly from $\{-1, 1\}$. Chips from different codes are independent.

The aggregate bit rate of the system is R_b so that the bit rate per base station is R_b/N, corresponding to a symbol duration NT_b. The corresponding chip duration is $T_c = NT_b/L_c$. The signal transmitted by the mth base station is

$$
s_m(t) = P_t \left(\sum_{k=-\infty}^{\infty} (2a_{mk} - 1)p(t) + 1 \right) \tag{41}
$$

$$
p(t) = \sum_{j=0}^{L_c-1} c_{kj}^{(n(m))} \Pi(\lambda_m(t,j,k)) \tag{42}
$$

$$
\lambda_m(t,j,k) = \frac{t - (kL_c + j)T_c - \Delta_m}{T_c} \tag{43}
$$

where the additive constant ensures that $s_m(t)$ is nonnegative.

At the receiver, the signal is convolved with a unit-energy filter matched to the chip-pulse shape, sampled at the chip rate, and then correlated against the proper chip sequence. Since the signal is symmetric about its average, the dc component can be ignored. We must now count all the base stations in the room—not just those using the same "channel" or code. We will assume that there are M total interferers under consideration, with N_I of them sharing the same code as the desired base station. Let $x_m = \lfloor \Delta_m/T_c \rfloor$ and $y_m = \Delta_m/T_c - x_m$. We observe that x_m takes on the values $0, \cdots, L_c - 1$ with probability $1/L_c$, that y_m is uniform on $[0, 1)$, and that x_m and y_m are independent. The decision metric for bit k from base station zero is then

$$
r_k = \sqrt{NT_bL_c} P_t \kappa H_0(\rho)(2a_{0k} - 1)
$$
$$
+ \sum_{m=1}^M \sqrt{NT_bL_c} P_t \kappa H_0(\rho_m) C_m + n_k \tag{44}
$$

$$
C_m = (2a_{m,k-1} - 1)y_m R_1(m, x_m)
$$
$$
+ (2a_{m,k-1} - 1)(1 - y_m) R_2(m, x_m)
$$
$$
+ (2a_{m,k} - 1)y_m R_3(m, x_m)
$$
$$
+ (2a_{m,k} - 1)(1 - y_m) R_4(m, x_m) \tag{45}
$$

$$
R_1(m, x_m) = \sum_{j=0}^{x_m} c_{k,j}^{(n(0))} c_{k-1,j+L_c-1-x_m}^{(n(m))} \tag{46}
$$

$$R_2(m, x_m) = \sum_{j=0}^{x_m-1} c_{k,j}^{(n(0))} c_{k-1,j+L_c-x_m}^{(n(m))} \qquad (47)$$

$$R_3(m, x_m) = \sum_{j=x_m+1}^{L_c-1} c_{k,j}^{(n(0))} c_{k,j-x_m-1}^{(n(m))} \qquad (48)$$

$$R_4(m, x_m) = \sum_{j=x_m}^{L_c-1} c_{k,j}^{(n(0))} c_{k,j-x_m}^{(n(m))}. \qquad (49)$$

Note that the noise shown here (n_k) is actually a sum of L_c independent chip noise samples, each of which is Gaussian distributed with mean zero and variance N_0. Thus, n_k is Gaussian with mean zero and variance $L_c N_0$. If r_k is positive, the receiver decides that a one was sent; otherwise, it decides that a zero was sent. The probability of bit error is

$$P_e = E\left[Q\left(\sqrt{S(\gamma)}\left[1 + \frac{1}{L_c} \sum_{m=1}^{N_I} \frac{H_0(\rho_m)}{H_0(\rho)} C_m \right] \right) \right] \qquad (50)$$

with

$$S(\gamma) = N H_0^2(\rho)\gamma \qquad (51)$$

where the expectation is taken over x_m, y_m, all pairs of bits $(a_{m,0}, a_{m,-1})$, and all possible sequence of code bits $c_{k,j}^{(n(m))}$, for $m = 1, \cdots, M$.

2) Direct-Sequence Spreading using Optical Orthogonal Codes: When CDMA is applied to fiber-optic systems, which typically employ data rates of 1–10 Gb/s, electronic despreading becomes difficult because of the high chip rate. Optical despreading offers a potential solution. In intensity-modulated systems, since intensity is nonnegative, it is necessary to employ spreading codes that consist only of zeroes and ones and have low periodic- and cross-correlation properties. The codes, which are known as OOC's [6], [13], [14], have also recently been proposed for infrared wireless systems [6].

An optical orthogonal code is a set of sequences of L_c bits that meet the following two conditions [13].

1) Any sequence $c_j, j = 0, \cdots, L_c - 1$ satisfies

$$\left| \sum_{j=0}^{L_c-1} c_j c_{j+1} \right| \begin{cases} = K & \text{for } l = 0 \\ \leq \lambda_a & \text{for } l = 1, \cdots, L_c - 1. \end{cases} \qquad (52)$$

2) Every pair of sequences $c_j^{(n)}$ and $c_j^{(m)}$ satisfies

$$\sum_{j=0}^{L_c-1} c_j^{(n)} c_{j+l}^{(m)} \leq \lambda_c \quad \text{for} \quad l = 0, \cdots, L_c - 1. \qquad (53)$$

Because we wish to minimize interference between base stations, and for numerical tractability, we restrict ourselves to the case where $\lambda_a = \lambda_c = 1$. For such codes, the number of available sequences N as a function of the number of ones in the code K and the number of chips in the code L_c is given by [13]

$$N \leq \left\lfloor \frac{L_c - 1}{K(K-1)} \right\rfloor. \qquad (54)$$

The analysis for CDMA using OOC is similar to that for m-sequences, except that now, the bit sequences and the signal are both sequences that take on the values zero and one. Again, the symbol duration is NT_b, and the chip duration is $T_c = NT_b/L_c$. The signal transmitted by the mth base station is

$$s_m(t) = \frac{P_t L_c}{K} \sum_{k=-\infty}^{\infty} a_{mk} p(t) \qquad (55)$$

$$p(t) = \sum_{j=0}^{L_c-1} c_{kj}^{(n(m))} \Pi(\lambda_m(t,j,k)) \qquad (56)$$

$$\lambda_m(t,j,k) = \frac{t - (kL_c + j)T_c - \Delta_m}{T_c}. \qquad (57)$$

At the receiver, the signal is convolved with a unit-energy filter matched to the chip pulse shape, sampled at the chip rate, and then correlated against the transmitted OOC sequence. Once again, we have M interfering base stations, with N_I of them sharing the same sequence as the desired base station. Let $x_m = \lfloor \Delta_m/T_c \rfloor$ and $y_m = \Delta_m/T_c - x_m$. Again, x_m takes on the values $0, \cdots, L_c - 1$ with probability $1/L_c, y_m$ is uniform on $[0, 1)$, and x_m and y_m are independent. The decision metric for bit k from base station zero is then

$$r_k = \sqrt{NT_b L_c} P_t \kappa H_0(\rho) a_{0k}$$
$$+ \sum_{m=1}^{N_I} \sqrt{NT_b L_c} P_t \kappa H_0(\rho_m) I_m + n_k \qquad (58)$$

$$I_m = a_{m,k-1} y_m R_1(m, x_m)$$
$$+ a_{m,k-1}(1 - y_m) R_2(m, x_m)$$
$$+ a_{m,k} y_m R_3(m, x_m)$$
$$+ a_{m,k}(1 - y_m) R_4(m, x_m) \qquad (59)$$

$$R_1(m, x_m) = \sum_{j=0}^{x_m} c_{k,j}^{(n(0))} c_{k-1,j+L_c-1-x_m}^{(n(m))} \qquad (60)$$

$$R_2(m, x_m) = \sum_{j=0}^{x_m-1} c_{k,j}^{(n(0))} c_{k-1,j+L_c-x_m}^{(n(m))} \qquad (61)$$

$$R_3(m, x_m) = \sum_{j=x_m+1}^{L_c-1} c_{k,j}^{(n(0))} c_{k-1,j-x_m-1}^{(n(m))} \qquad (62)$$

$$R_4(m, x_m) = \sum_{j=x_m}^{L_c-1} c_{k,j}^{(n(0))} c_{k-1,j-x_m}^{(n(m))}. \qquad (63)$$

The only contributions to the decision metric from signal, noise, and interference are the chips during which the desired OOC sequence takes on the value of one. Therefore, the n_k are i.i.d. Gaussian with mean zero and variance KN_0. Since the r_k form a set of i.i.d. random variables, we can define a threshold $D = E[r_k]$. If r_k is above the threshold, the receiver decides that a one was sent; otherwise, it decides that a zero was sent.

In [13] and [14], the authors use two probabilistic models that can be used to calculate an upper and lower bound for the probability of bit error. These models are based on the weak chip-asynchronous and the chip-synchronous assumptions, respectively.

a) Weak Chip-Asynchronous Assumption: As the time off-set of an interfering transmission changes, the amount of interference caused by that transmission changes. Under the weak chip-asynchronous assumption [13], we assume that for different code sequences, no more than a single one from each sequence can overlap at a given time offset, and for the same code sequence, no more than a single one from the transmitted sequence overlaps with the correlating sequence unless $x_m = 0$. The probability density function of I_m as $a_{m,k}, a_{m,k-1}, x_m$, and y_m vary is then

$$f_{I_m}(v) = \left(1 - \frac{K^2}{L_c}\right)\delta(v) + \frac{K^2}{L_c}\Pi\left(v - \frac{1}{2}\right) \quad (64)$$

for $n(m) \neq n(0)$, and

$$f_{I_m}(v) = \left(1 - \left(\frac{K^2 - K + 1}{L_c}\right)\right)\delta(v)$$
$$+ \frac{1}{KL_c}\Pi\left(\frac{v - \frac{K}{2}}{K}\right)$$
$$+ \frac{K(K-1)}{L_c}\Pi\left(v - \frac{1}{2}\right) \quad (65)$$

for $n(m) = n(0)$. The resulting probability of bit error is given by

$$P_e = \frac{1}{2}E\left[Q\left(\sqrt{S(\gamma)}\left[1 + \frac{2}{K}\sum_{m=1}^{M}\frac{H_0(\rho_m)}{H_0(\rho)}C_m\right]\right)\right]$$
$$+ \frac{1}{2}E\left[Q\left(\sqrt{S(\gamma)}\left[1 - \frac{2}{K}\sum_{m=1}^{M}\frac{H_0(\rho_m)}{H_0(\rho)}C_m\right]\right)\right] \quad (66)$$

$$S(\gamma) = \frac{NL_cH_0^2(\rho)\gamma}{4K} \quad (67)$$

$$C_m = \frac{K^2}{2L_c} - I_m \quad (68)$$

where the expectation is taken over C_m for $m = 1, \cdots, M$.

b) Chip-Synchronous Assumption: Under the chip-synchronous assumption, we assume that whenever an interfering code sequence is correlated against the desired sequence, the correlation takes on the maximum possible value [13]. If the interfering and desired sequences are different elements of the OOC, then this value is one when x_m is such that two nonzero chips overlap and zero otherwise. When the interfering and desired sequences are the same, this value is K when $x_m = 0$, one when $x_m \neq 0$ and two nonzero chips overlap, and zero otherwise. The probability density function for I_m under this assumption is

$$f_{I_m}(v) = \frac{K^2}{2L_c}\delta(v - 1) + \left(1 - \frac{K^2}{2L_c}\right)\delta(v) \quad (69)$$

for $n(m) \neq n(0)$, and

$$f_{I_m}(v) = \frac{K^2 - 1}{2L_c}\delta(v - 1) + \frac{1}{2L_c}\delta(v - K)$$
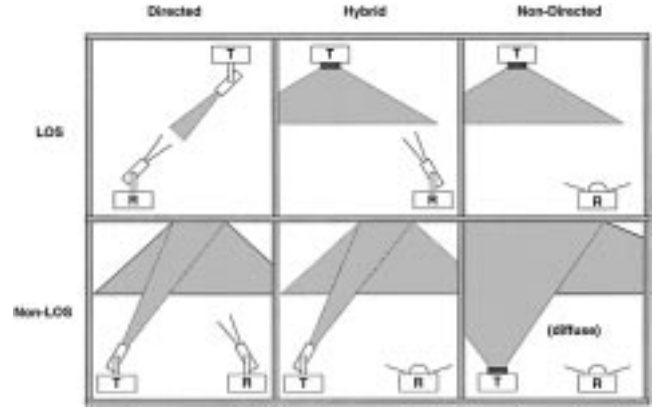$$+ \left(1 - \frac{K^2}{2L_c}\right)\delta(v) \quad (70)$$

Fig. 2. Configurations for wireless infrared links. Nondirected, non-line-of-sight, or diffuse systems are considered here.

for $n(m) = n(0)$. In this distribution, interferers contribute differently to the decision threshold depending on whether they use the same code as the desired base station or not. We assume that base stations 1 to N_I share the code of the desired base station and that base stations $N_I + 1$ to M use different codes. The resulting probability of bit error is

$$P_e = \frac{1}{2}E\left[Q\left(\sqrt{S(\gamma)}\left[1 + \frac{2}{K}\sum_{m=1}^{N_I}\frac{H_0(\rho_m)}{H_0(\rho)}C_m\right]\right)\right]$$
$$+ \frac{1}{2}E\left[Q\left(\sqrt{S(\gamma)}\left[1 - \frac{2}{K}\sum_{m=1}^{N_I}\frac{H_0(\rho_m)}{H_0(\rho)}C_m\right]\right)\right] \quad (71)$$

$$S(\gamma) = \frac{NL_cH_0^2(\rho)\gamma}{4K} \quad (72)$$

$$C_m = \begin{cases} \dfrac{K^2 + K - 1}{2L_c} - I_m & \text{for } 1 \leq m \leq N_I \\[2mm] \dfrac{K^2}{2L_c} - I_m & \text{for } N_I + 1 \leq m \leq M. \end{cases} \quad (73)$$

where the expectation is taken over I_m for $m = 1, \cdots, M$.

III. PERFORMANCE COMPARISONS

There are several configurations possible for indoor wireless infrared links, as shown in Fig. 2. A transmitter and receiver may have a narrow radiation pattern or field of view, respectively, and can be combined to make directed, nondirected, or hybrid systems. Systems may also be classified as line-of-sight (LOS) or nonline-of-sight (non-LOS), depending on whether or not they rely on the existence of a direct path between transmitter and receiver. The two most common configurations are directed, LOS links and nondirected, non-LOS links (which are commonly referred to as *diffuse* links). Directed LOS links have several advantages, which include minimal path loss, received ambient light, and multipath distortion. However, such links require careful aiming, making them unsuitable for mobile terminals. Furthermore, such links can be degraded significantly by shadowing. In this work, we have chosen to study diffuse links because they combine ease of use with robustness against shadowing [4].

TABLE I
VARIATION OF $S(\gamma)$ WITH RESUSE STRATEGY. IN THE
NOISE-LIMITED CASE, THE BER IS PROPORTIONAL TO
$Q(\sqrt{S(\gamma)})$. γ IS THE SNR FOR UNIT OPTICAL PATH GAIN

| Reuse Strategy	$S(\gamma)$
TDMA/OOK	$N^2 H_0^2(\rho)\gamma$
TDMA/2^L-PPM	$N^2 2^{L-1} L H^2_0(\rho)\gamma$
FDMA/BPSK	$\dfrac{N H_0^2(\rho)\gamma}{2C^2(\alpha)}$
FDMA/QPSK	$\dfrac{N H_0^2(\rho)\gamma}{2C^2(\alpha)}$
CDMA/m-sequence	$N H_0^2(\rho)\gamma$
CDMA/OOC	$\dfrac{N L_c H_0^2(\rho)\gamma}{4K}$

In each reuse scheme we have considered, the BER consists of terms of the form $E[Q(\sqrt{S(\gamma)}[1 + I])]$. In the noise-limited regime, the BER is determined by $S(\gamma)$, i.e., the BER is proportional to $Q(\sqrt{S(\gamma)})$. Table I provides $S(\gamma)$ for each reuse and modulation scheme studied. The parameter I determines how much the performance is degraded by cochannel interference. The quantity I is of the form of a weighted sum of $H_0(\rho_m)/H_0(\rho)$, which is the ratio of the optical path gain to the user from interfering base station m to the gain from the desired base station. The BER will decrease as the optical signal-to-interference ratio (SIR)

$$\text{SIR} = \frac{H_0(\rho)}{\displaystyle\sum_{m=1}^{M} H_0(\rho_m)} \qquad (74)$$

increases.

One common way to achieve channel reuse is to assign fixed channels using a cellular scheme [8]. A room is broken up into hexagonal cells, and each cell is assigned a different channel. Fig. 3(a) illustrates this idea for a system using three channels. Each cell would have a transmitter at its center, pointed at the ceiling to produce a diffuse configuration. For any base station, the six closest base stations using the same channel are known as nearest neighbors. The location of the first nearest neighbor is specified using the coordinate axes shown in Fig. 3(b), and the rest are determined from symmetry. If the "first" nearest neighbor is located at coordinates (k, l) and R_c is the radius of a cell as measured from its center to a vertex, then the number of channels needed for this system is given by the reuse factor $N = k^2 + l^2 + kl$, and the distance between a cell and its nearest neighbors is given by the reuse distance $K = \sqrt{3N}R_c$ [8]. In Fig. 3(a), the first nearest neighbor is located at $(1, 1)$, the reuse factor is $N = 3$, and nearest neighbors are separated by $D = 3R_c$.

We have measured the path loss for a diffuse system as a function of the horizontal separation between transmitter and receiver in several different rooms. A typical example, which was taken in an open-plan office approximately 6.9×43.4 m
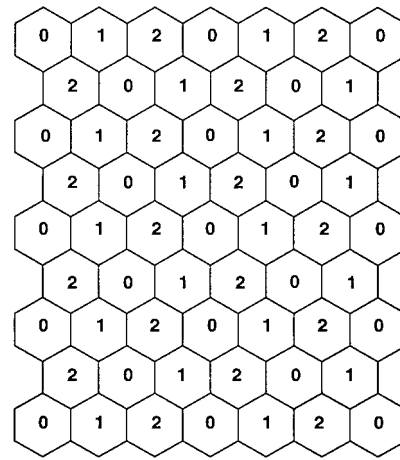
(a)
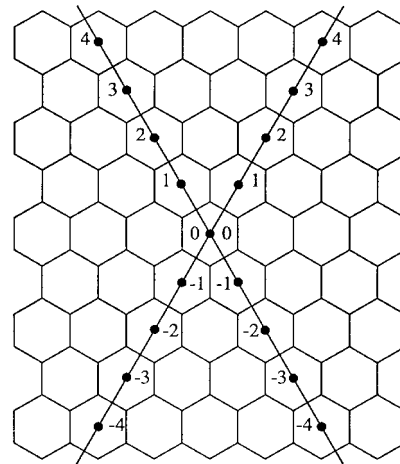
(b)

Fig. 3. Basic cellular geometry. (a) Assignment of channels for a cellular system with a reuse factor of three. (b) Axes used to specify the position of a cell relative to a desired base station in a system using hexagonal cells.

with a 2.7 m ceiling, is shown in Fig. 4(a). The office was filled with cubicles. A transmitter was placed in the middle of a cubicle, and a receiver was moved along a line bisecting the wall of the cubicle. $H_0(\rho)$ was approximated from this data by a function of the form

$$H_0(\rho) = \frac{1}{a_0 + a_1\rho + a_2\rho^2 + a_3\rho^3 + \rho^4}. \qquad (75)$$

The fitted curve, which is shown in Fig. 4(a), minimizes the mean-square difference between the logarithms of the measured data and fitted curves. To improve the shape of the fit, an extra data point, shown filled in black in Fig. 4(a), was extrapolated from the data and added near the origin. This fitted function is used in all performance estimates below.

The worst-case position in any cell is clearly that point at which the SIR (74) is smallest. For the chosen gain function and for $H_0(\rho)$ corresponding to any well-designed transmitter radiation pattern, this is a vertex of the cell. The worst-case SIR for these systems is shown in Fig. 4(b). For cell radii greater than 4 m, the worst-case SIR exceeds 10, and we say
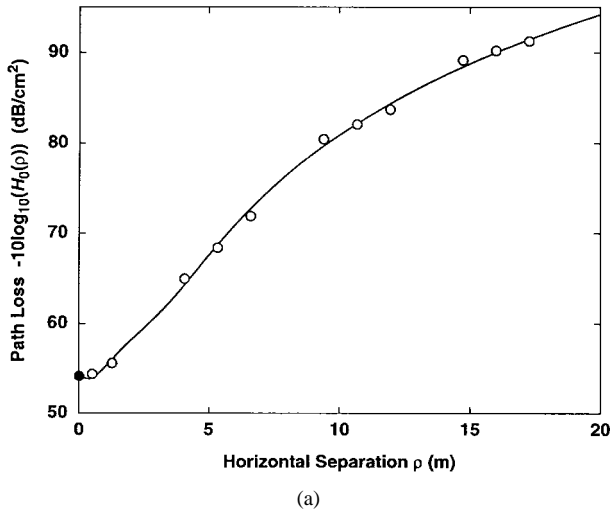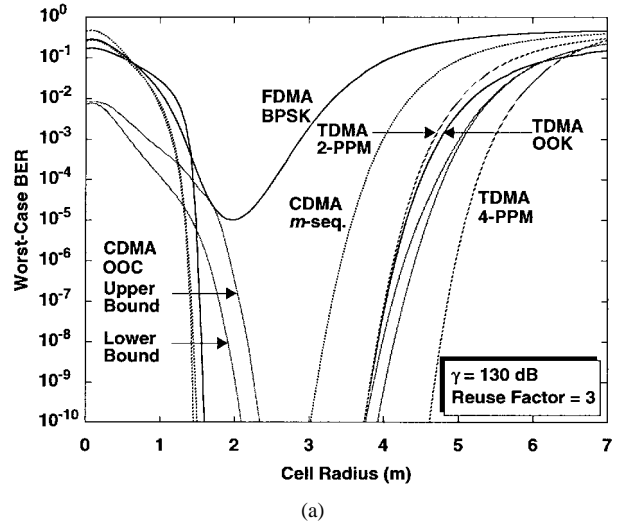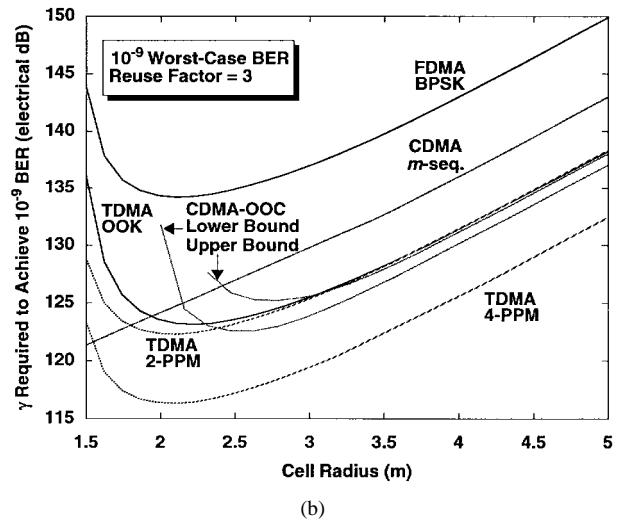
(a)
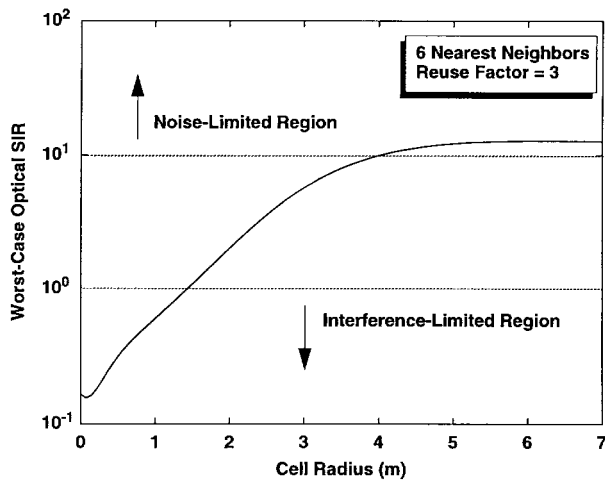
(b)

Fig. 4. (a) Path loss $-10\log_{10}(H_0(\rho))$ versus ρ in a diffuse infrared link. Open circles represent measured points, the solid curve represents a fitted curve, and the filled-in point was added to improve the fit. (b) Optical SIR at the vertex of a hexagonal cell as a function of cell radius considering only the six nearest neighbors computed using the fitted path-loss curve.

(a)

(b)

Fig. 5. Performance comparisons assuming hexagonal cells with a reuse factor of three. (a) Worst-case bit-error rate as a function of cell radius for six reuse schemes with $\gamma = 130$ dB. (b) Value of γ required to achieve a worst-case bit-error rate of 10^{-9} as a function of cell radius for six reuse schemes. The curves for CDMA with an OOC assume a code with $K = 9$ and $L_c = 217$. The curve for CDMA with m-sequences assumes $L_c = 16$.

that the system is noise limited. For cell radii below 1.5 m, the worst-case interference can be larger than the desired signal, and we declare the system to be interference limited.

Fig. 5(a) shows the worst-case bit error rate in a cell as a function of the cell radius using $\gamma = 130$ dB, a first nearest neighbor at $(1, 1)$, and a reuse factor of $N = 3$ for the different channel reuse methods discussed above. In order to improve computational efficiency, the BER's were computed using moment-generating functions [15] derived from the decision metrics given in Section II. The moment-generating functions and their derivation can be found in [16]. For TDMA systems, we consider use of OOK, 2-PPM, and 4-PPM. For FDMA, we consider a BPSK system using pulses with excess bandwidth $\alpha = 1$. In these two systems, cochannel interference arises only from base stations using the same channel as the desired system, and only the six nearest neighbors are considered. We consider the maximum and minimum cell radii of the system to be the largest and smallest radii, respectively, for which we can achieve a worst-case BER of 10^{-9}.

In Fig. 5(a), we see that for $\gamma = 130$ dB, 2-PPM and OOK have essentially the same performance in the noise-limited region, achieving a maximum cell radius of approximately 3.8 m, whereas using 4-PPM increases this to 4.7 m. In the interference-limited region, the minimum cell radius for 2-PPM and 4-PPM is 1.5 m, which is slightly better than the 1.6 m achieved by OOK. FDMA using BPSK is the worst performer in all regions, due largely to the dc offset required in its implementation. It never achieves a BER of 10^{-9} for any cell radius. QPSK has not been shown here because of the complexity required to compute its BER. However, it is clear from (38)–(40) that its performance in a noise-limited situation would be the same as for BPSK, and its performance would be worse than for BPSK in an interference-limited case.

For CDMA, we assume only N codes were available for use. In Fig. 5(a), BER performance is shown for m-sequences with $L_c = 16$ and for an OOC with $K = 9$ and $L_c = 217$, which is the smallest possible choice permitting equality in

(54). Unlike the other systems, all cells within the ring of nearest neighbors are considered to be interferers. This means that at a cell vertex, there are always at least two cells whose received powers are equal to the power of the desired transmitter. With m-sequences, CDMA achieves a maximum cell radius of just over 3.1 m, which is considerably smaller than for TDMA with OOK. However, the BER of CDMA for this case is always noise limited; therefore, its minimum cell radius is 0 m, despite the fact that we have used only N codes. The maximum cell radius of CDMA using an OOC is between 3.7 and 3.9 m, and the minimum cell radius is between 2.1 and 2.3 m. Thus, in a noise-limited situation, it performs somewhat better than OOK, yet in an interference-limited environment, only FDMA performs worse for this case.

We recall that γ equals the SNR for unit optical path gain and is proportional to the square of the transmitted optical average power. Fig. 5(b) shows the value of γ required to achieve a worst-case BER of 10^{-9} for cell radii between 1.5 and 5 m for a cellular reuse pattern with the first nearest neighbor at (1, 1) and a reuse factor of $N = 3$. In the noise-limited regime, i.e., for cell radii above 3 m, TDMA with OOK and 2-PPM and CDMA using an OOC all require approximately the same γ. Using TDMA with 4-PPM results in a 6-dB decrease in the required value of γ. Conversely, CDMA using m-sequences requires an increase in γ of 5 dB over TDMA using OOK, and FDMA with BPSK and $\alpha = 1$ requires an increase of 12 dB. These differences in performance are largely attributable to the differences in $S(\gamma)$ among the various reuse and modulation schemes. For simplicity, we have considered $N = 3$, which represents the smallest realistic reuse factor. We recall that the noise-limited BER is proportional to $Q(\sqrt{S(\gamma)})$ for all schemes. Examining Table I, we see that in the noise-limited regime, as N is increased, the required value of γ decreases inversely with N^2 for TDMA schemes and inversely with N for FDMA and CDMA schemes.

In Fig. 5(b), we see that as the cell radius decreases, cochannel interference causes an increase in the value of γ required to achieve a worst-case BER of 10^{-9}. TDMA, FDMA, and CDMA using an OOC eventually reach a point where cochannel interference produces an irreducible BER greater than 10^{-9}. For TDMA and FDMA strategies, this occurs at a cell radius near 1.5 m, and for CDMA using an OOC, it occurs between 2 and 2.25 m. The poor performance of CDMA using an OOC is due, in part, to the reuse of codes. Increasing the number of codes without changing the bit rate (R_b/N per base station) or the parameter K results in a higher value of L_c and decreases the radius at which the irreducible BER occurs. For any particular radius, this method leads to a lower value of L_c than increasing L_c and/or K without changing the number of codes. For CDMA with m-sequences, increasing the value of L_c does not change the SNR, but it does decrease the effect of other user interference. Thus, with m-sequences, there is a limit to the benefits of increasing L_c. For $L_c = 16$, other-user interference is reduced to the point that the BER of CDMA with m-sequences is determined by $S(\gamma)$ at all reasonable cell radii and does not result in an irreducible BER at any practical cell radius. Thus, for cell radii below approximately 1.5 m, CDMA using m-sequences always requires the lowest value of γ.

Based on the above, we conclude that for cell radii above 1.5 m, TDMA using 2^L-PPM provides distinct advantages over other channel reuse schemes, both in optical average power required and in ease of implementation. For cell radii below 1.5 m, CDMA using m-sequences presents a power advantage, but this is likely to be offset by increased complexity. For such small cells, if it is permissible to have "dead zones" between regions covered by different base stations, then use of short-range, LOS links may provide sufficient connectivity with decreased complexity.

IV. CELLULAR NETWORK DESIGN EXAMPLE

As an example, we consider a very large open-plan office having many cubicles, and each is 3.75 m square and with four occupants. The receiver translates received irradiance to photocurrent with a constant $\kappa = 1.18\,\mathrm{cm^2 A/W}$ (corresponding to an optical gain of 3.17, a filter transmission of 68%, detector area of 1 cm^2, and photodetector responsivity of 0.55). The receiver is assumed to employ an optical bandpass filter having a 30-nm-wide passband. Windows admit bright skylight, which induces shot noise, resulting in a white Gaussian noise of two-sided density $N_0 = 6.6 \times 10^{-23}\,\mathrm{A^2/Hz}$. Because of its demonstrated efficiency, we employ TDMA. We choose an aggregate bit rate of $R_b = 30$ Mb/s. We choose OOK over PPM because of the greater immunity of the former technique to multipath ISI at this high bit rate [10]. Our objective is to provide an average bit rate of 2 Mb/s per user with a worst-case BER of 10^{-9} while maximizing peak throughput and minimizing the required number of transmitters.

Minimizing the number of transmitters used is equivalent to maximizing the cell size. This, and the fact that we wish to maximize the peak throughput, indicates that we should use the lowest reuse factor possible. The lowest feasible reuse factor for a TDMA system is $N = 3$, where the first nearest neighbor is located at (1, 1). Since we have four users per cubicle with an area of 14 m^2 per cubicle, in order to provide an average of 2 Mb/s per user, we need to achieve a data density of approximately 0.142 Mb/(s $-$ m^2). The area of a hexagonal cell is given by $A = \sqrt{27}R^2/2$; therefore, the maximum desirable cell radius is 3 m. From Fig. 5(b), we find that this requires a γ of approximately 125 dB. This implies that an average transmitter power of 70.5 mW is required.

Since the peak bit rate of each transmitter is 30 Mb/s, multipath effects must be taken into account [4]. It is also necessary to consider the effects of shadowing. At a cell radius of 3 m, the system is largely noise limited. Therefore, a decision feedback equalizer (DFE) that minimizes mean-squared error can be used to compensate for ISI due to multipath without needing to consider the added cochannel interference. We can then compensate for multipath by increasing the transmitter power by 1.8 dB [4]. Neglecting cochannel interference, in a diffuse system, shadowing increases the path loss by 3 dB while producing only marginal changes in the ISI penalty [4]. If we consider the worst case of only shadowing the path from the desired base station, we can calculate that an

increase in γ by 7.6 dB will compensate for the increased path loss due to shadowing. This corresponds to a 3.8-dB increase in transmitter power. An examination of the BER formula for TDMA with OOK indicates that increasing the transmitter power does not affect the interference level. Thus, when OOK is used, a transmitter with an average power of 257 mW will provide adequate performance in the presence of both multipath and shadowing. The base stations should be placed in the center of cells of 3 m radius. The proper geometry and time slot assignment are indicated in Fig. 3(b).

V. CONCLUSIONS

We have examined systems of fixed-channel reuse for base stations in an indoor infrared wireless communications system. The systems compared include TDMA using OOK and PPM, FDMA using BPSK and QPSK, and CDMA using m-sequences and an OOC. We defined a parameter γ, which equals the SNR for unit optical path gain and is proportional to the square of the average transmitted optical power. Using measured path-loss data, it was found that in a system using hexagonal cells and a reuse factor of three, for cell radii above 3 m, TDMA with OOK and 2-PPM and CDMA using an OOC all require approximately the same γ to achieve a worst-case BER in the cell of 10^{-9}. Using TDMA with 4-PPM results in a 6-dB decrease in the required γ. Conversely, CDMA using m-sequences requires an increase in γ of 5 dB over TDMA using OOK, and FDMA with BPSK using pulses with excess bandwidth $\alpha = 1$ requires an increase of 12 dB. As the reuse factor N increases, in the noise-limited regime, the required value of γ decreases in inverse proportion to N^2 for TDMA schemes and inversely with N for FDMA and CDMA schemes. For cell radii below 3 m, cochannel interference dominates the systems using TDMA, FDMA, and CDMA with an OOC. This results in an irreducible BER greater than 10^{-9} at cell radii less than 1.5 m for the TDMA and FDMA systems examined. The irreducible BER occurs at approximately 2 m for CDMA with an OOC, but this can be reduced by increasing the spreading factor or increasing the number of codes used. Only CDMA with m-sequences does not develop an irreducible BER, making it the only choice for cell radii below 1.5 m. However, for such small cell radii, cellular reuse schemes may not be desirable.

ACKNOWLEDGMENT

REFERENCES

[1] F. R. Gfeller and U. H. Bapst, "Wireless in-house data communication via diffuse infrared radiation," *Proc. IEEE*, vol. 67, pp. 1474–1486, Nov. 1979.
[2] J. R. Barry, *Wireless Infrared Communications*. Boston: Kluwer, 1994.
[3] J. M. Kahn *et al.*, "Non-directed infrared links for high capacity wireless LAN's," *IEEE Pers. Commun. Mag.*, vol. 1, pp. 12–25, May 1994.
[4] J. M. Kahn, W. J. Krause, and J. B. Carruthers, "Experimental characterization of nondirected indoor infrared channels," *IEEE Trans. Commun.*, vol. 43, pp. 1613–1623, Feb.–Mar.–Apr. 1995.
[5] R. T. Valadas, J. M. Brázio, and A. M. de Oliveira Duarte, "Throughput performance of nonpersistent CSMA/CD quasidiffuse infrared local area networks under an imperfect average power sensing collision detection method," in *Proc. Int. Conf. Commun.*, vol. 1, May 1993, pp. 567–572.
[6] J. M. H. Elmirghani and R. A. Cryan, "Indoor infrared LAN's with multiple access facilities based on hybrid PPM CDMA," in *Proc. Int. Conf. Commun.*, vol. 2, June 1995, pp. 731–734.
[7] F. R. Gfeller, P. Bernasconi, W. Hirt, C. Elisii, and B. Weiss, "Dynamic cell planning for wireless infrared in-house data transmission," in *Proc. Int. Zurich Seminar Digital Commun.*, Mar. 1994, pp. 261–272, .
[8] V. H. Mac Donald, "The cellular concept," *Bell Syst. Tech. J.*, vol. 58, no. 1, pp. 15–42 Jan. 1979.
[9] J. G. Proakis, *Digital Communications, 3rd ed.* New York: McGraw-Hill, 1995.
[10] M .D. Audeh and J. M. Kahn, "Performance evaluation of L-pulse position modulation on nondirected indoor infrared channels," in *Proc. Int. Conf. Commun.*, vol. 2, May 1994, pp. 660–664.
[11] J. B. Carruthers and J. M. Kahn, "Multiple-subcarrier modulation for nondirected wireless infrared communication," *IEEE J. Select Areas Commun.*, vol. 14, pp. 538–546, Apr. 1996.
[12] M. K. Simon, J. K. Omura, R. A. Scholtz, and B. K. Levitt, *Spread Spectrum Communications Handbook, Revised Edition*. New York: McGraw-Hill, 1994.
[13] J. A. Salehi, "Code division multiple access techniques in optical fiber networks—Part I: Fundamental principles," *IEEE Trans. Commun.*, vol. 37, pp. 824–833, Aug. 1989.
[14] J. A. Salehi and C. A. Brackett, "Code division multiple access techniques in optical fiber networks—Part II: Systems performance Analysis," *IEEE Trans. Commun.*, vol. 37, pp. 834–842, Aug. 1989.
[15] C. W. Helstrom, "Calculating error probabilities for intersymbol and cochannel interference," *IEEE Trans. Commun.*, vol. COM-34, pp 430–435, May 1986.
[16] G. W. Marsh, "High-speed wireless infrared communication links," Ph.D. dissertation, Univ. California, Berkeley, Dec. 1995.

Gene Marsh (M'84) received the B.S. degree in computer science and electrical engineering from Rose-Hulman Institute of Technology, Terre Haute, IN, in 1985, the M.S. degree in electrical engineering from Stanford University, Stanford, CA, in 1987, and the Ph.D. in electrical engineering from the University of California, Berkeley, in 1995. His Ph.D. thesis was entitled "High-Speed Wireless Infrared Communication Links."

He is currently employed as a systems engineer at Qualcomm, Incorporated, San Diego, CA.

Joseph M. Kahn (M'87) received the A.B., M.A., and Ph.D. degrees in physics from the University of California, Berkeley (U.C. Berkeley), in 1981, 1983, and 1986, respectively. His Ph.D. thesis was entitled "Hydrogen-Related Acceptor Complexes in Germanium."

From 1987 to 1990, he was a Member of Technical Staff in the Lightwave Communications Research Department, AT&T Bell Laboratories, Crawford Hill Laboratory, Holmdel, NJ, where he performed research on multigigabit-per-second coherent optical fiber transmission systems and related device and subsystem technologies. He demonstrated the first BPSK-homodyne optical fiber transmission system and achieved world records for receiver sensitivity in multigigabit-per-second systems. He joined the faculty of U.C. Berkeley in 1990, where is currently a Professor with the Department of Electrical Engineering and Computer Sciences. His research interests include infrared and radio wireless communications and optical fiber communications.

Dr. Kahn is a recipient of the National Science Foundation Presidential Young Investigator Award and is a member of the IEEE Communications Society and IEEE Lasers and Electro-Optics Society. He is serving currently as a technical editor for IEEE PERSONAL COMMUNICATIONS MAGAZINE.